Neuronal couplings between retinal ganglion cells inferred by efficient inverse statistical physics methods

Simona Cocco[a,1], Stanislas Leibler[b,c], and Rémi Monasson[d]

[a]Laboratoire de Physique Statistique de l'Ecole Normale Supérieure, Université Pierre et Marie Curie, Université Denis Diderot, Centre National de la Recherche Scientifique, 24 Rue Lhomond, 75005 Paris, France; [b]Center for Studies in Physics and Biology and Laboratory of Living Matter, The Rockefeller University, 1230 York Avenue, New York, NY 10065; [c]The Simons Center For Systems Biology and School of Natural Sciences, Institute for Advanced Study, Einstein Drive, Princeton, NJ 08540; and [d]Laboratoire de Physique Théorique de l'Ecole Normale Supérieure, Université Pierre et Marie Curie, Centre National de la Recherche Scientifique, 24 Rue Lhomond, 75005 Paris, France

Communicated by Roderick MacKinnon, The Rockefeller University, New York, NY, June 18, 2009 (received for review February 15, 2009)

Complexity of neural systems often makes impracticable explicit measurements of all interactions between their constituents. Inverse statistical physics approaches, which infer effective couplings between neurons from their spiking activity, have been so far hindered by their computational complexity. Here, we present 2 complementary, computationally efficient inverse algorithms based on the Ising and "leaky integrate-and-fire" models. We apply those algorithms to reanalyze multielectrode recordings in the salamander retina in darkness and under random visual stimulus. We find strong positive couplings between nearby ganglion cells common to both stimuli, whereas long-range couplings appear under random stimulus only. The uncertainty on the inferred couplings due to limitations in the recordings (duration, small area covered on the retina) is discussed. Our methods will allow real-time evaluation of couplings for large assemblies of neurons.

inference and inverse problems | multielectrode recordings | neural couplings

A vertebrate retina is a structured, complex network of interacting neurons that process visual input stimuli at the photoreceptors into an output pattern of action potentials of the retinal ganglion cells (1–2). It is now a well-established fact that retinal cells process information in a collective fashion: The firing of one ganglion cell is correlated with the firing pattern of other cells (3–4). Multielectrode recordings have made accessible hours-long, simultaneous spiking activity of tens of retinal ganglion cells and thus have become a powerful tool to investigate the information processing performed by a vertebrate retina (5–7). The analysis of pairwise correlations in the activity has revealed different patterns of synchrony between 2 cells that have been related to different retina circuits (7).

Analyzing the concerted activity of all of the recorded cells is, however, a very challenging task. Recently Schneidman et al. (8) and Shlens et al. (9) pointed out that correlations in the firing activity of cell populations can be reconstructed from the average firing rates, f_i, and 2-cell correlations, c_{ij}, alone. The theoretical model, which has been used to generate the frequencies of all possible 2^N spiking configurations for a system of N neurons, is the well-known Ising model. It is characterized by a reduced set of $\approx N^2$ parameters: N "fields," h_i, experienced by individual cells, and $N(N-1)/2$ "couplings," J_{ij}, between pairs of cells. Computing the parameters h_i and J_{ij} from the firing patterns can be viewed as an example of the inverse statistical physics method.

The existence of a low-dimensional parameterization of the retinal activity (8–11) is an interesting and encouraging result. Naively, one may be tempted to assign to the inferred parameters a simple interpretation: The fields could represent the external stimuli, and the couplings could reflect the physiological interactions between the cells. However, because most of the neural circuitry (all cells in intermediate layers and most of the cells in the ganglion layer) is not recorded, the inferred fields and couplings are only "effective" quantities, and many questions remain unanswered. First, how do the effective couplings depend on the visual stimulus? Second, to what extent are the inferred couplings affected by the incomplete sampling of the activity, both from temporal (finite duration of the recordings) and spatial (small area of the retina covered by the electrode array) points of views? Third, do the couplings strongly depend on the model used for the inference? The main difficulty in addressing these questions in a systematic manner is connected with the computational complexity of the applied inverse statistical algorithm.

In the present work, we propose 2 efficient algorithms to calculate the effective couplings from the spiking activity of a population of neurons. The first method is based on the above-mentioned Ising model, the second one on the well-known "leaky integrate-and-fire" (I&F) model. We then use these algorithms to characterize the effective couplings between ganglion cells from previously published recordings of the salamander retinal activity under different visual stimuli.

Results

Ising and I&F Models. Existing algorithms for inverse Ising problems are based on time-consuming learning schemes (11–12). It is possible, however, to drastically improve inverse Ising methods if one takes advantage of the fact that the neurons are more often silent than active. This situation corresponds to the behavior of the Ising model at high fields. Based on a high-field expansion of the Ising thermodynamic potential at fixed f_i and c_{ij}, we have developed an efficient algorithm, which calculates the couplings, as well as their relative accuracy, in a time polynomial in N [*Methods* and supporting information (SI) *Appendix*, Section 1]. This means in practice that for a typical recording of the activity of $N = 32$ ganglion cells in the salamander retina, $N(N-1) \approx 10^3$ couplings can be inferred (on a personal computer) in a couple of minutes rather than in many hours.

The Ising approach takes into account correlations in the "same time bin" (of the order of 20 ms) but completely ignores time-delayed correlations. We have thus developed a second approach based on the I&F model (13–15) (*Methods* and *SI Appendix*, Section 3). I&F is a dynamical model describing spike generation by a neuron in the presence of the synaptic inputs from other neurons; couplings are pairwise but are not a priori

Author contributions: S.C., S.L., and R.M. designed research, performed research, contributed new reagents/analytic tools, analyzed data, and wrote the paper.

The authors declare no conflict of interest.

[1]To whom correspondence should be addressed. E-mail: cocco@lps.ens.fr.

This article contains supporting information online at www.pnas.org/cgi/content/full/0906705106/DCSupplemental.

symmetric. Using techniques from statistical field theory, we have devised an efficient inference procedure for calculating the couplings, G_{ij}, from all of the S recorded spikes, in a time polynomial in both N and S. For the recording mentioned above ($S \approx 10^5$ spikes) the running algorithm time is of the order of 20 s on a personal computer.

As an example of potential application, we reanalyze 3 recordings from salamander ganglion cells: (*i*) a 2,000-s-long recording of the spontaneous activity of 32 cells in total darkness (5); (*ii*) a 4,450-s-long recording of the same 32 cells in the same retina illuminated with randomly flickering bright squares (5) (the locations of the receptive field centers of those cells are known); and (*iii*) a recording from 40 cells in another retina presented with a 120-s-long natural movie repeated 20 times (8).

Both the Ising and I&F models are approximations to the real neural activity. We have checked that multicell correlations, calculated in the Ising model within the same time bin, are rather faithfully reproduced, although slightly overestimated (*SI Appendix*, Section 2). The I&F model, on the other hand, despite its simplicity, is capable of reproducing some important features of the longer-time correlations between spiking events (*SI Appendix*, Section 4).

Correlations Versus Interactions. The task of inferring couplings from the dataset is more complex than the long-established process of analyzing correlations in the firing activity (3–7). The coupling between 2 cells is indeed not only a function of the activity of the pair itself but depends on the activity of all of the recorded cells. It is, however, interesting to compare the couplings inferred through the Ising model and the correlation indices (*Methods*) previously defined (6) in the analysis of multielectrode array data (see *SI Appendix*, Section 4). The logarithm of the correlation index is the first contribution to the Ising coupling in our large-field expansion. This 2-cell approximation to the coupling corresponds to calculating the coupling only from the average firing rates and correlation of the 2 cells in the pair (see *Methods*). As shown in Fig. 1, some Ising couplings J_{ij} can be accurately approximated from their 2-cell approximation. In general, however, the coupling between 2 cells cannot be deduced directly from the correlation of their firing activities, because this correlation may result from indirect couplings via other neurons. By adding the consecutive expansion terms to this 2-cell approximation, one can systematically generalize the correlation index analysis by including correlations within the larger clusters of cells (*Methods*). We have found that pairs of cells with positive and large correlation indices have, in general, large couplings with values close to their 2-cell approximation, whereas pairs with positive and small correlation indices may have negative couplings (*SI Appendix*, figure 5). The presence of negative couplings is an interesting finding that cannot be deduced from the analysis of the data in terms of correlations (see histogram of couplings, and of their 2-cell approximations in *SI Appendix*, figures 3 and 4).

Note that the difference between couplings and correlations indices and the size of the clusters of cells necessary for an accurate inference depend, in general, on the structure of the neural circuit.

Comparison of Couplings Obtained in Dark and Flicker Conditions. Although the cell activities are different in flicker and dark conditions, many pairs have similar Ising couplings J_{ij} in both conditions (Fig. 2); this is the case both for strong positive couplings (such as pair "a," whose cells often spike together within a time window $\Delta t = 20$ ms), and for several negative couplings (e.g., pair "b," showing no correlation). Note, however, that few large and positive couplings under flicker stimulus have small or even negative values in dark (e.g., pair "'c," with a strong correlation in flicker and anticorrelation in dark), and few positive couplings in the dark have negative values under flicker conditions (e.g., pair "d," whose cells are positively correlated but with a long delay >20 ms). The difference of behaviors of pairs a, b, c, and d between the 2 stimuli presumably correspond to different classes of physiological interactions, as appears from the full-time histogram of cross-correlations.

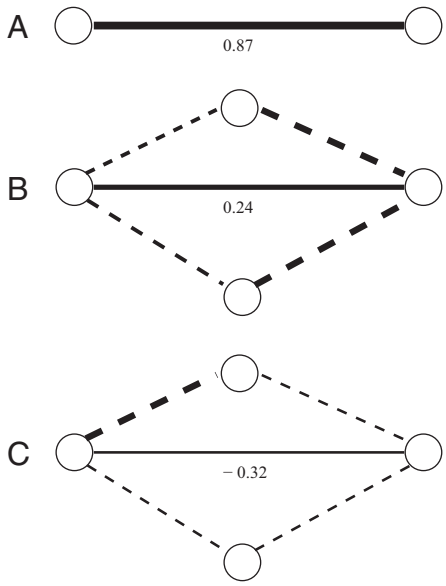

Fig. 1. Network of couplings responsible for the measured correlations. Interaction paths in 3 selected pairs of cells *i*,*j* with positive correlations c_{ij}, among 32 cells recorded under flicker stimulus (data courtesy of M. Meister, ref. 5). Direct couplings are represented by full lines, indirect couplings by dashed lines. Line widths are proportional to the intensities of the couplings they carry (couplings <0.3 in absolute value are omitted). The fraction of the correlation c_{ij} because of the direct coupling J_{ij} is indicated for each pair. (*A*) A direct, strong, and positive interaction between the 2 cells of the pair accounts for most of the measured correlation. The 2-cell contribution to coupling, $J_{ij}^{(2)} = (\log CI_{ij})/4$, where CI_{ij} is the so-called correlation index (*Methods* and ref. 7) is $J_{ij}^{(2)} = 0.66$, an accurate approximation to the true coupling, $J_{ij} = 0.70$. (*B*) A substantial fraction of the correlation between the 2 cells of the pair results from strong, positive interactions through other cells. The coupling cannot be approximated from the correlation index: For this pair $J_{ij}^{(2)} = 0.8$, whereas $J_{ij} = 0.5$. To obtain the correct value of the coupling, our expansion must take into account subsets with 4 cells at least (*Methods*). (*C*) Extreme case of positively correlated cells with a strong, negative direct interaction. The positive correlation between the 2 cells of the pair results from several interaction paths going through 1 or more other cells. For this pair $J_{ij}^{(2)} = 0.3$ whereas $J_{ij} = -0.3$.

Comparison Between I&F and Ising Couplings. The presence of numerous strong positive couplings is corroborated by the I&F analysis (Fig. 3). In the I&F model, G_{ij} is rarely equal to G_{ji}, but the couplings are grouped along the symmetry axis. Overall asymmetry of couplings is larger in dark than in flicker conditions (Fig. 3 and *SI Appendix*) The symmetrized I&F interactions $(G_{ij} + G_{ji})/2$ are proportional to positive Ising couplings J_{ij}, but the agreement between the Ising and I&F models is poorer for negative couplings, especially under flicker stimuli, because the Ising model ignores correlations with delays larger than Δt (e.g., pair d of Fig. 2). We find this discrepancy to be particularly important for structured stimuli, such as natural movie, which generally lead to larger delays in the spiking activity (Fig. 3).

Dependence of Couplings on Removal of Cells from the Recordings. Multicellular recordings of neurons interrogate only a small portion of retinal ganglion cells. To study how restricting the number of measured neurons affects the inferred couplings, we

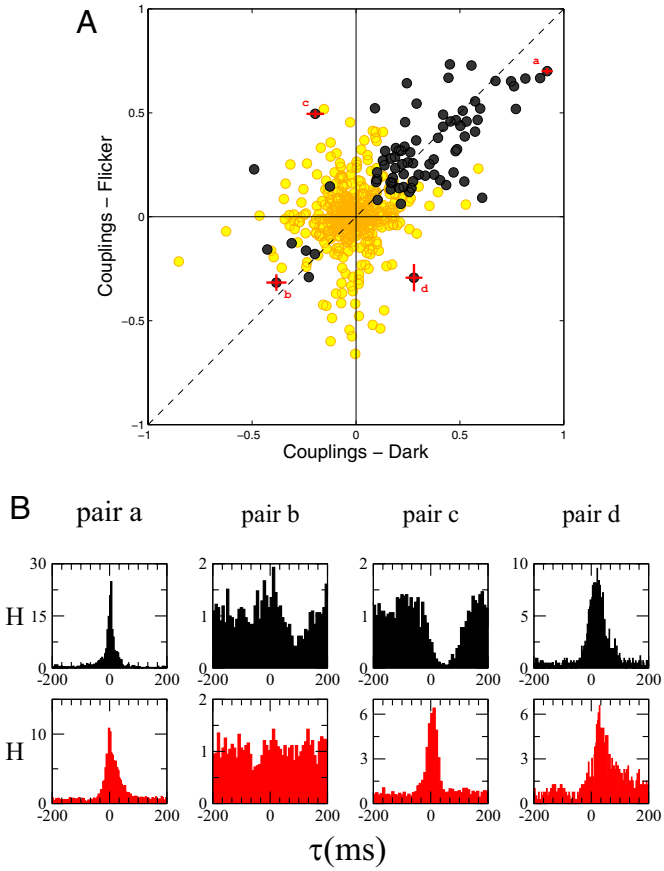

Fig. 2. Ising couplings and cross-correlation histograms for dark and flicker stimuli. (*A*) Dependence of Ising couplings J_{ij} on visual stimulus. Activities of 32 cells were recorded in dark and under flicker stimuli on the same retina (data courtesy of M. Meister). The uncertainty of the coupling values, because of the limited amount of recorded data, can be calculated by using the inverse Ising algorithm (see *SI Appendix*, Section 1); the couplings, for which the relative uncertainty is <30%, are depicted in black (called "reliable"), all others ("unreliable") in yellow. The figure shows a comparison of couplings in dark versus in flicker for all cell pairs (*i*,*j*). Bin size is $\Delta t = 20$ ms. Statistical errors are exemplified for 4 pairs of cells (marked in red and labeled a–d). Strong positive couplings are more reliable because the 2 cells spike often during the recorded interval. (*B*) Cross-correlation histograms for pairs a–d of *A*. Histograms of the delays between spiking times of the cell pairs a–d recorded in dark (black) and flicker conditions (red). Pair a: The 2 cells in dark and flicker often spike together within a few tens of milliseconds. Pair b: Absence of correlation between the activity of the 2 cells both in flicker than in dark. Pair c: Negative correlation in the dark and positive correlation in flicker in a time window of some tens of milliseconds. Pair d: Positive correlations with a delay of ≈20 ms in dark and 40 ms in flicker.

"removed" a portion of the recorded cells and recalculated J_{ij}. Within a linear response approximation, the removal of a cell does not change couplings beyond 600 μm (the data are limited to distances <1.4 mm). However, couplings are often affected by removal, or inclusion, of nearby cells (*SI Appendix*, Sections 6 and 7). We conclude that in order for the couplings between central cells to be reliable, the electrode arrays have to be dense enough (with spacing typically <40 μm) and have to probe most ganglion cells in a surrounding region >1 mm.

Dependence of Couplings on Distance Between Cells. Fig. 4 shows the Ising and I&F couplings between pairs of ganglion cells as a function of the distance between their receptive field centers for dark and flicker conditions. The analyzed recordings do not lead to any clear dependence of the couplings on the cell type, probably because most recorded cells (80%) are of the OFF type. We therefore group all cells together, independently of their type. The results are compatible with the conclusions of Meister et al. (6) based on the study of pairwise correlations. The dependences of the Ising and I&F couplings on distance are very similar, although, as explained in Fig. 3, the Ising negative couplings have larger amplitudes than the I&F couplings. We observe that whereas strong positive couplings are found at small distances (<500 μm) both in dark and flicker conditions, the positive couplings at larger distances (up to 1,000 μm) exist mainly in flicker but not in dark conditions and are hence stimulus induced. At the same time, negative couplings, including the few conserved interactions identified above, are acting at distances >200 μm. The absence of negative interactions at short distances in dark and in flicker conditions could come from the homogeneity in the recorded cell types.

Spatial Networks of Couplings. Spatial information about the couplings can be depicted in form of 2D maps in the retinal plane obtained by connecting the receptive field centers with lines representing the couplings. Remarkably, the maps of the strongest couplings obtained with the I&F and the Ising inverse statistical approaches include largely the same pairs of cells (Fig. 5). The map of the strongest couplings in dark conditions (Fig. 5 *A* and *C*) has a simple connectivity: with short-range couplings between neighboring cells. In contrast, the strong interactions present in flicker and absent in dark (e.g., pair c) are long range (Fig. 5 *B* and *D*). The appearance of these couplings seems to be at odds with recent studies in primate retina, which have found that the quasitotality of the informational entropy of spikes can be accounted for by assuming only interactions between adjacent cells (9).

Discussion

We have presented 2 computationally efficient inverse statistical approaches, thereby establishing a solid basis for the rapid, low-dimensional parameterization of neural activity. We have classified the inferred couplings with respect to their sign, dependence on the stimulus, on the inference model, and their spatial range. Although most pairwise correlations are positive, both the Ising and I&F models predict the existence of negative couplings, which can be long range and stimulus dependent. In addition to the stimulus-dependent couplings, we have located strong, positive, short-range couplings, which are similar both in the dark and under flicker stimuli.

A crucial issue connected with this low-dimensional parameterization of neural activity remains: Can the effective couplings J_{ij} be given a simple physiological interpretation (2)? For instance, it will be important to explore the physiological meaning of the long-range couplings, which appear under flicker stimuli, and could be, e.g., mediated by amacrine cells. It would be also interesting to see whether symmetric I&F couplings correspond to direct interactions between neurons (e.g., via gap junctions) (7). Additional physiological measurements could be performed to explore the underlying nature of the interneuronal couplings.

Most of the inferred couplings are expected to reflect the effective interactions through the intermediate retina layers, which are not easily accessible to measurement and the circuitry of which cannot be reconstructed (1–2). Yet, effective couplings between ganglion cells could give important insights on the way the retina encodes and transmits visual information. The computational efficiency of our inverse statistical approaches should make possible experiments in which the couplings are calculated in real time, while the firing activity is being recorded. Visual stimuli could be adjusted during experiments to explore particular aspects of retinal function. This possibility is not restricted only to multielectrode recordings in vertebrate retina: The same approach could be also used to analyze the activity of other

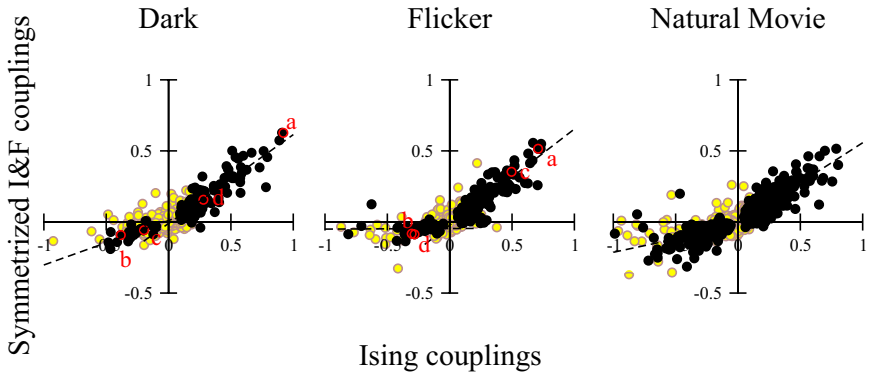

Fig. 3. Symmetrized I&F couplings ($G_{ij} + G_{ji}$)/2 versus Ising couplings J_{ij} for dark (*Left*), flicker (*Middle*), and natural move (*Right*) conditions. Reliable couplings are depicted in black, unreliable in yellow; red labels refer to the same 4 cell pairs as in Fig. 2. Solid lines represent the best linear fits for positive and negative reliable couplings. For positive couplings, a linear relationship is well verified for the 3 conditions with the same slope (of ≈0.6). The slope depends on the parameters of the models such as the time bin Δt for Ising model and the membrane leak conductance g of the I&F model (here Δt = 20 ms, g = 0). See *SI Appendix*, Section 5 for a calculation of the slopes, as a function of Δt. Negative couplings are characterized by a linear fit with different slopes; moreover, in flicker and natural movie conditions, couplings display a larger dispersion around the linear fit. The difference between the slopes for positive and negative couplings and the larger dispersion for negative couplings can be understood by considering the distributions of the delays between spikes (*SI Appendix*, Section 4). Pairs of cells with positive couplings often fire pairs of correlated spikes separated by a few tens of milliseconds (e.g., pair c in flicker, and pair a in both flicker and dark, see Fig. 2), whereas the separation is typically larger for negatively coupled cells (e.g., pair d in flicker), especially in flicker and natural move conditions. Thus, the I&F model (here with the leak conductance g = 0) takes into account all temporal correlations for both positively and negatively coupled cells, whereas the Ising model (here with Δt = 20 ms) does it only in the former case.

neuronal systems, such as the recordings from slices of vertebrate cortex (12).

Methods

Algorithm for the Inverse Ising Problem. Data are encoded into bit configurations: $s_i^\tau = 1$ if cell i is active in bin τ, 0 otherwise, where time bins are of width Δt; $\tau = 1,2,\ldots,B$ is in the index of the time bin in the recording of duration $B \times \Delta t$. In the Ising model, the log-likelihood of a N-bit configuration (in the same bin) is

$$\log P^{\text{like}}(s_1, s_2, \ldots, s_N | \{h_i\},\{J_{ij}\}) = 2 \sum_i h_i s_i + 4 \sum_{i<j} J_{ij} s_i s_j + F[\{h_i\},\{J_{ij}\}], \quad [1]$$

where the parameters h_i and J_{ij} are called, respectively, effective fields and couplings; the value of $F[\{h_i\},\{J_{ij}\}]$, called free energy in statistical physics, is such that the probabilities of the 2^N configurations sum up to 1. The effective fields and couplings must be inferred to reproduce the experimentally measured average activities, $p_i = \langle s_i \rangle$, where $p_i = f_i \times \Delta t$ is the probability that cell i fires in a bin, and cell–cell correlations, $p_{ij} = \langle s_i s_j \rangle$ here $\langle \cdot \rangle$ denotes the average, with the probability P^{like}. Those equations are ill defined because of imperfect sampling, e.g., J_{ij} would be infinite if cells i and j never spike together in the set of B configurations. To avoid this problem, we introduce a Gaussian prior over the parameters and infer the effective fields and couplings through the maximization of the Bayesian log-posterior probability

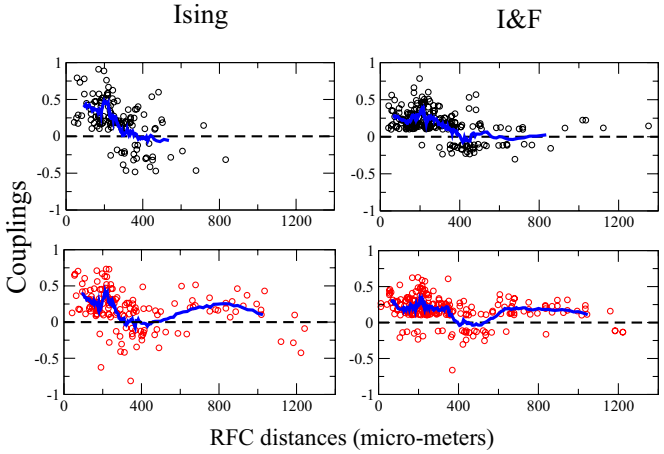

Fig. 4. Ising and I&F couplings versus distance. Couplings as a function of the distance between receptive field centers in dark (black) and flicker (red) conditions inferred from the Ising (*Left*) and I&F (*Right*) models. Only Ising couplings J_{ij} with relative error <30% and I&F couplings G_{ij} and G_{ji} with absolute values <0.1 are shown. Negative couplings are absent at short distances (<200 μm) in dark and flicker conditions, and positive couplings are rare in dark at large distances (>500 μm). Blue lines represent the moving averages over the 15 nearest points.

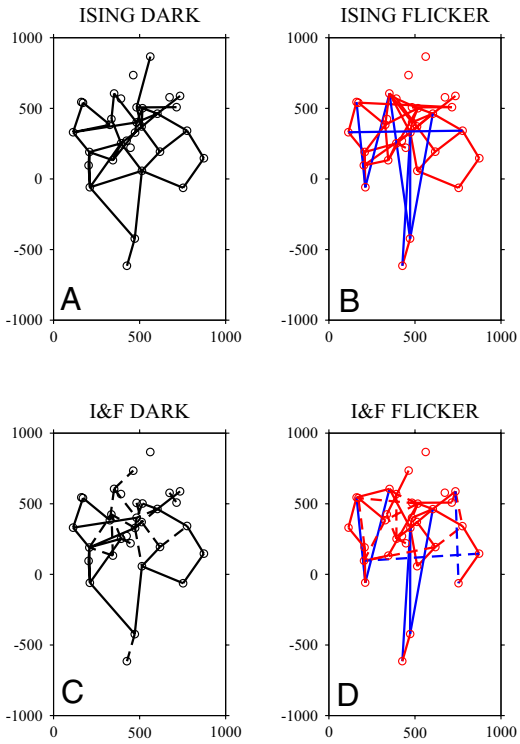

Fig. 5. Spatial maps of large positive couplings for Ising and I&F models. Links are connecting the receptive field centers (indicated by circles) of the 32 cells in dark (black) and in flicker (red). Distances are measured in microns. Shown here are the maps obtained from the largest couplings in the Ising and I&F models. (*A* and *B*) For the Ising model, links are drawn between pairs of cells (i,j) with couplings $J_{ij} > J_0 = 0.3$ in dark (40 links) (*A*) and flicker (48 links) (*B*). (*C* and *D*) The I&F maps contain the same numbers of largest couplings G_{ij} or G_{ji} to facilitate the visual comparison in dark (*C*) and flicker (*D*) conditions. Asymmetric couplings, such that $|G_{ij} - G_{ij}|/|G_{ij} + G_{ij}| > 0.3$, are shown with dashed lines. Long-range couplings (range >500 μm) are shown in blue; they are present in flicker, but absent in the dark. Maps of weak or negative couplings have a very different structure, see *SI Appendix*, Section 6.

PHYSICS

NEUROSCIENCE

$$\log P^{\text{post}}(\{h_i\},\{J_{ij}\}) = 2\sum_i h_i p_i + 4\sum_{i<j} J_{ij}p_{ij} + F[\{h_i\},\{J_{ij}\}] - \frac{\Gamma}{2}\left(\sum_i h_i^2 + \sum_{i<j} J_{ij}^2\right), \quad [2]$$

where Γ is expected to be of the order of $1/B$ (*SI Appendix*, Section 1).

Because the calculation of the free energy F, Eq. **1**, for a given set of fields and couplings requires a computational effort growing exponentially with the number N of cells, P^{post} cannot be directly maximized from the definition (Eq. **2**) when N exceeds, say, 15. Fortunately, we need to know F for large fields only: The firing probability p_i is small because the bin width Δt (≈20 ms) is much smaller than the average interspike interval (>1 s for dark and flicker recordings). We have extended large-field expansions existing in statistical physics to: (*i*) tackle the case of nonuniform (cell-dependent) couplings and fields, and (*ii*) perform the minimization over the (large) fields and the couplings in Eq. **2** to express F in terms of the firing probabilities p_i and correlations p_{ij}.

The outcome of the procedure is that the coupling J_{ab} can be decomposed into a sum of contributions coming from all clusters of $k+2$ distinct cells including cells a and b,

$$J_{ab}[\{p_i\},\{p_{ij}\}] = \sum_{k=0}^{N-2} \sum_{i_i<i_2<\ldots<i_k} J_{ab}^{(k+2)}[a,b,i_1,i_2,\ldots,i_k;\{p_i\},\{p_{ij}\}]. \quad [3]$$

The first term in the expansion is $J_{ab}^{(2)} = \frac{1}{4}\log CI_{ab}$, where $CI_{ab} = p_{ab}/(p_a p_b)$ is the correlation index of cells a and b (*SI Appendix*, Section 1) and is called here the 2-cell approximation to the coupling. Terms with $k \geq 1$ correspond to network contributions to J_{ab}: Informally speaking, $J_{ab}^{(k+2)}[a,b,i_1,i_2,\ldots,i_k]$ is the contribution to the coupling between cells a and b that cannot be obtained from the knowledge of the activities of smaller subsets of those $k+2$ cells.

Our expression for $J_{ab}^{(k+2)}[a,b,i_1,i_2,\ldots,i_k]$ is an infinite series in powers of the connected correlation $c_{ij} - p_i p_j$. Although we are not able to obtain a closed analytical expression we can show the following fact. Assume that all firing probabilities are small, that is, $p_i < \varepsilon$, for some small positive ε. Then the contribution from a cluster of $k+2$ cells to the effective coupling J_{ab} is of the order of ε^k and decreases very quickly with k. This property allows us to truncate the sum in Eq. **2**. In practice, we numerically sum up the series and calculate the contributions to the couplings coming from all clusters with $k+2 \leq 7$ cells. A similar procedure gives the expansion of the fields h_i.

Notice that the above algorithm not only provides us with the most likely values for the couplings and fields but also with the uncertainty on those values because of the finite number of recorded data. The error estimates for the couplings are obtained from the inverse of the Hessian matrix of $\log P^{\text{post}}$ (Fisher information matrix), see *SI Appendix*, Section 1.

Algorithm for the Inverse I&F Problem. In the I&F model, the membrane potential of each cell obeys the following equation,

$$C\frac{dV_i}{dt} = -gV_i + I^{\text{syn}} + I_i + \eta_i, \quad [4]$$

where g is the leak conductance of the membrane, C is the capacitance, I^{syn} is the current because of synaptic inputs from the other registered cells,

$$I^{\text{syn}}(t) = \sum_{j(\neq i)} G_{ij} \sum_l K(t - t_{jl}), \quad [5]$$

where t_{jl} is the time at which cell j emits its lth spike. The integration kernel $K(t)$ vanishes for $t < 0$ (causality) and for $t > t_s$ where t_s is the synaptic integration time; the integral of K over the $[0;t_s]$ interval is normalized to unit. The synaptic strength G_{ij}, which may be positive or negative, measures the overall change in the potential of cell i resulting from a spike emitted by cell j. The current coming from the other cells is modeled as a white noise process, with average value I_i, and Gaussian fluctuations

$$\langle \eta_i(t) \rangle = 0, \langle \eta_i(t)\eta_j(t') \rangle = \sigma^2 \delta_{ij}\delta(t - t') \quad [6]$$

uncorrelated from cell to cell. When the potential V_i exceeds the threshold value V_{th}, cell i emits a spike and the potential is reset to its rest value (equal to 0). Up to a rescaling of the couplings and currents we can set $V_{\text{th}} = C = 1$ without loss of generality; g can then be interpreted as the inverse of the leaking time of the membrane.

Eqs. **4**-**6** implicitly define the likelihood $P[\{t_{jl}\}|\{G_{ij},I_i\}]$ that our population of N neurons emit spikes at times $\{t_{jl}\}$ given the couplings G_{ij} and the average currents I_i. In the absence of a priori probability on the couplings and currents, the most likely values for the latter is found through the maximization of P. In principle, P can be calculated through the resolution of many Fokker–Planck equations, one for each spike in the dataset, associated to 1-dimensional Ornstein–Uhlenbeck processes with moving boundaries. In practice, this approach and related numerical approximations (15) are inadequate to process datasets with hundreds of thousands of spikes.

We have, therefore, resorted to an approximation for P, asymptotically exact when the amplitude σ of the synaptic noise Eq. **6** tends to zero: P is then dominated by the contribution coming from particular trajectories $V_i^*(t)$ of the potentials, called classical paths in physics (16) and optimal paths in large-deviation theory (17). The difficulty in finding the optimal potentials $V_i^*(t)$ consists in determining whether and when they touch the threshold (without crossing it) at intermediate times $t \neq t_{ik}$ (18). We have devised a fast and analytical procedure to calculate the optimal potentials, and thus the probability P, for a population of coupled cells, see *SI Appendix*, Section 3. As the likelihood P is a convex function of G_{ij} and I_i the couplings and currents with maximal probability are easily found by using a local ascent procedure, e.g., the Newton–Raphson algorithm, see *SI Appendix*, Section 3.

The procedure is able to determine $N \times (N-1)$ couplings and N currents from S spikes in a computational time scaling as $S \times N^2$. The algorithm has been tested on artificially generated data from networks with known couplings and currents with up to $N = 160$ cells and $S = 10^7$ spikes. The inferred couplings are largely independent on the initial conditions over the potentials used in the I&F simulation. For moderate noise levels, the interactions are correctly inferred, with error bars of the order of $1/\sqrt{S}$.

ACKNOWLEDGMENTS. M. Meister and M. Berry kindly made their multielectrode recordings available to us. We thank them for discussions and encouragement. We benefited from discussions with C. Bargmann, D. Butts, T. Holy, S. Kuehn, B. Knight, and R. Yuste and from their comments on our manuscript.

1. Field GD, Chichilnisky E (2007) Information processing in the primate retina: Circuitry and coding. *Annu Rev Neurosci* 30:1–30.
2. Hosoya T, Baccus SA, Meister M (2005) Dynamic predictive coding by the retina. *Nature* 436:71–77.
3. Arnett DW (1978) Statistical dependence between neighboring retinal ganglion cells in goldfish. *Exp Brain Res* 32:49–53.
4. Mastronarde DN (1989) Correlated firing of retinal ganglion cells. *Trends Neurosci* 12:75–80.
5. Schnitzer MJ, Meister M (2003) Multineuronal firing patterns in the signal from eye to brain. *Neuron* 37:499–511.
6. Meister M, Lagnado L, Baylor DA (1995) Concerted signaling by retinal ganglion cells. *Science* 270:1207–1210.
7. Brivanlou IH, Warland DK, Meister M (1998) Mechanisms of concerted firing among retinal ganglion cells. *Neuron* 20:527–539.
8. Schneidman E, Berry M, Segev R, Bialek W (2006) Weak pairwise correlations imply strongly correlated network states in a neural population. *Nature* 440:1007–1012.
9. Shlens J, et al. (2006) The structure of multi-neuron firing patterns in primate retina. *J Neurosci* 26:8254–8266.
10. Nirenberg S, Victor J (2007) Analyzing the activity of large populations of neurons: Low tractable is the problem? *Curr Opin Neurobiol* 17:397–400.
11. Tkacik G, Schneidman E, Berry MJ, II, Bialek W (2006) Ising models for networks of real neurons. *arXiv* q-bio.NC, 0611072.
12. Tang A, et al. (2008) A maximum entropy model applied to spatial and temporal correlations from cortical networks in vitro. *J Neurosci* 28:505–518.
13. Stein RB (1965) A theoretical analysis of neuronal variability. *Biophys J* 5:173–194.
14. Burkitt AN (2006) A review of the integrate-and-fire neuron model. *Biol Cybern* 95:1–19 and 97–112.
15. Paninski L, Pillow JW, Simoncelli EP (2004) Maximum likelihood of a stochastic integrate-and-fire neural encoding model. *Neural Comput* 16:2553.
16. Zinn-Justin J (2003) *Path Integrals in Quantum Mechanics* (Oxford Univ Press, Oxford).
17. Dembo A, Zeitouni O (1993) *Large Deviation Techniques and Applications* (Springer, Berlin), 2nd Ed.
18. Paninski L (2006) The most likely voltage path and large-deviation approximations for integrate-and-fire neurons. *J Comput Neurosci* 21:71.